HHS Public Access

Author manuscript

Angiogenesis. Author manuscript; available in PMC 2023 February 11.

Published in final edited form as:

Angiogenesis. 2023 February ; 26(1): 77–96. doi:10.1007/s10456-022-09852-7.

Protein disulfide isomerase A1 as a novel redox sensor in VEGFR2 signaling and angiogenesis

Sheela Nagarkoti[1], **Young-Mee Kim**[1,7], **Dipankar Ash**[1], **Archita Das**[1], **Eric Vitriol**[5], **Tracy-Ann Read**[5], **Seock-Won Youn**[1,8,9], **Varadarajan Sudhahar**[1,6], **Malgorzata McMenamin**[1,6], **Yali Hou**[1,6], **Harriet Boatwright**[1], **Ruth Caldwell**[1,4,6], **David W. Essex**[10], **Jaehyung Cho**[11,12], **Tohru Fukai**[1,3,6], **Masuko Ushio-Fukai**[1,2]

[1]Vascular Biology Center, Medical College of Georgia at Augusta University, 1460 Laney-Walker Blvd, Augusta, GA 30912, USA

[2]Department of Medicine (Cardiology), Medical College of Georgia at Augusta University, Augusta, GA 30912, USA

[3]Departments of Pharmacology and Toxicology, Medical College of Georgia at Augusta University, Augusta, GA, USA

[4]Vision Discovery Institute, Medical College of Georgia at Augusta University, Augusta, GA, USA

[5]Neuroscience and Regenerative Medicine, Medical College of Georgia at Augusta University, Augusta, GA, USA

[6]Charlie Norwood Veterans Affairs Medical Center, Augusta, GA 30912, USA

[7]Department of Medicine (Cardiology), University of Illinois at Chicago, Chicago, IL, USA

[8]Department of Physiology and Biophysics, University of Illinois at Chicago, Chicago, IL, USA

[9]Center for Cardiovascular Research, University of Illinois at Chicago, Chicago, IL, USA

[10]Department of Medicine, Temple University School of Medicine, Philadelphia, PA, USA

[11]Division of Hematology, Department of Medicine, Washington University School of Medicine, St. Louis, MO, USA

[12]Department of Pathology and Immunology, Washington University School of Medicine, St. Louis, MO, USAz

Abstract

✉Masuko Ushio-Fukai, mfukai@augusta.edu.

Sheela Nagarkoti, Young-Mee Kim: equally contributed first author.

Author contributions MU-F, TF, SN, Y-MK, designed the study; SN, Y-MK, DA, VS, SWY, YH, AD, EV, TAR performed experiments. MM, HB, performed mouse genotyping. MU-F, TF, SN and Y-MK, DA, AD, analyzed data. VS, RC, DWE, JC, discussed data and provided inputs and reagents. MU-F, TF, SN, Y-MK, wrote the manuscript. RC, DWE, JC. edited the manuscript. All authors read and approved the final version of the manuscript.

Supplementary Information The online version contains supplementary material available at https://doi.org/10.1007/s10456-022-09852-7.

Conflict of interest The authors declare no competing financial interests.

Ethical approval The animal protocols used in this study were approved by the institutional Animal Care Committee and institutional Biosafety Committee of University of Illinois at Chicago and Augusta University.

VEGFR2 signaling in endothelial cells (ECs) is regulated by reactive oxygen species (ROS) derived from NADPH oxidases (NOXs) and mitochondria, which plays an important role in postnatal angiogenesis. However, it remains unclear how highly diffusible ROS signal enhances VEGFR2 signaling and reparative angiogenesis. Protein disulfide isomerase A1 (PDIA1) functions as an oxidoreductase depending on the redox environment. We hypothesized that PDIA1 functions as a redox sensor to enhance angiogenesis. Here we showed that PDIA1 co-immunoprecipitated with VEGFR2 or colocalized with either VEGFR2 or an early endosome marker Rab5 at the perinuclear region upon stimulation of human ECs with VEGF. PDIA1 silencing significantly reduced VEGF-induced EC migration, proliferation and spheroid sprouting via inhibiting VEGFR2 signaling. Mechanistically, VEGF stimulation rapidly increased *Cys-OH* formation of PDIA1 via the NOX4–mitochondrial ROS axis. Overexpression of "redox-dead" mutant PDIA1 with replacement of the active four Cys residues with Ser significantly inhibited VEGF-induced PDIA1–CysOH formation and angiogenic responses via reducing VEGFR2 phosphorylation. $Pdia1^{+/-}$ mice showed impaired angiogenesis in developmental retina and Matrigel plug models as well as ex vivo aortic ring sprouting model. Study using hindlimb ischemia model revealed that PDIA1 expression was markedly increased in angiogenic ECs of ischemic muscles, and that ischemia-induced limb perfusion recovery and neovascularization were impaired in EC-specific Pdia1 conditional knockout mice. These results suggest that PDIA1 can sense VEGF-induced H_2O_2 signal via CysOH formation to promote VEGFR2 signaling and angiogenesis in ECs, thereby enhancing postnatal angiogenesis. The oxidized PDIA1 is a potential therapeutic target for treatment of ischemic vascular diseases.

Keywords

Protein disulfide isomerase A1; Angiogenesis; Vascular endothelial cell growth factor; Redox signaling; Endothelial cell

Introduction

Reactive oxygen species (ROS) such as H_2O_2 derived from NADPH oxidases (NOXs) or superoxide dismutases (SODs) functions as signaling molecules to mediate biological responses [1–5]. Angiogenesis, a new vessel formation from the pre-existing ones, is essential for wound repair and treatment of ischemic heart and limb disease. Vascular endothelial growth factor (VEGF) binding to VEGF receptor type 2 (VEGFR2/Flk1) on the plasma membrane induces receptor dimerization and autophosphorylation. This results in internalization to $Rab5^+$ early endosomes to activate the sustained VEGFR2 signaling and angiogenic responses, such as proliferation, migration and capillary tube formation of endothelial cells (ECs) [6, 7]. We and others reported that H_2O_2 plays an important role in VEGFR2 signaling and angiogenic responses in ECs and postnatal neovascularization in vivo [1–3]. Recently, we showed that "ROS-induced ROS release" orchestrated by NOX4, NOX2 and mitochondria promotes VEGFR2 signaling and angiogenesis in ECs [8, 9]. However, how the NOX–mitochondrial ROS (mitoROS) signaling axis modulates active specific redox signaling to enhance therapeutic angiogenesis is poorly understood. The redox signaling is characterized by reversible oxido-reductive modifications, confined both spatially and temporally in subcellular compartments [10, 11]. The signaling function of

ROS is mainly mediated through reversible oxidation of reactive cysteine (Cys) residues (SH (thiol)) in target proteins to form “cysteine sulfenic acid (Cys-OH, sulfenylation)”, which is important for disulfide bond formation and redox signaling [10, 12, 13]. Little is known about how redox target proteins which often have low intrinsic reactivity towards H_2O_2 can be specifically and efficiently oxidized by VEGF-induced ROS.

Protein disulfide Isomerases (PDIs) functions as endoplasmic reticulum (ER) chaperones and thiol oxidoreductases that catalyze thiol oxidation, reduction or isomerization, depending on the cellular redox environment [14, 15]. PDI is universally expressed and has at least 21 family members in mammals [14]. PDI is present mainly in the ER but is also found in the cytosol, mitochondria and on the cell surface [14, 15]. PDIA1 is a major PDI isoform with the two a/a’ thioredoxin-like redox active (CysGlyHisCys) motifs that have four reactive Cys residues (C53,56,397,400), two b/b’ substrate binding motifs and C-terminal ER retention sequence (KDEL) [14–16]. Global Pdia1 knockout (KO) mice are embryonic lethal [17]. Of note, reduced form of PDI functions as a reductase while oxidized form of PDIA1 functions as an oxidase to promote disulfide bond formation with specific substrates to regulate their function [15]. In quiescent ECs, we previously reported that PDIA1 function as a thiol reductase for mitochondrial fission protein Drp1 to maintain normal mitochondrial and endothelial function [18]. PDIA1 is shown to be required for NOX activation to increase ROS in vascular smooth muscle cells (VSMCs) and macrophage [15, 19]. However, the role of endothelial PDIA1 in ROS-dependent VEGF signaling and postnatal angiogenesis in *vivo* is unknown.

In the present study, using $Pdia1^{\pm}$ mice and endothelial-restricted Pdia1 conditional knockout ($PDIA1^{ECKO}$) mice, we provide evidence that endothelial PDIA1 plays an important role in postnatal developmental and reparative angiogenesis in vivo. In cultured ECs, VEGF stimulation increased the physical association or colocalization of PDIA1 with VEGFR2 at $Rab5^{+}$ early endosomes as well as promoting PDIA1–CysOH formation through NOX4- and mitoROS-dependent manners. PDIA1 depletion or overexpression of “redox-dead” mutant PDIA1 with replacement of the active four Cys residues with Ser (PDIA1–CS) inhibited angiogenic responses via reducing p-VEGFR2 and VEGFR2 downstream signaling. Thus, PDIA1 functions as a redox sensor that transmits VEGF-induced NOX4–mitoROS signal axis via sulfenylation, thereby driving angiogenic responses in ECs.

Materials and methods

Animals

All animal studies were carried out following protocols approved by the institutional Animal Care Committee and institutional Biosafety Committee at University of Illinois at Chicago and Augusta University. Room temperature and humidity were maintained at 22.5 °C and between 50 and 60%, respectively. All mice were held under the 12:12 (12-h light: 12-h dark) light/dark cycle. Mice were held in individually ventilated caging with a maximum of 5 or a minimum of 2 mice per cage. C57BL/6 (control, wild type (WT)) and $Pdia1^{+/-}$ mice [20] were used at p5 (5 days after the birth) (for retina angiogenesis model) and at 8–12 weeks (for hindlimb ischemia model). EC-specific Pdia1 knockout ($Pdia1^{ECKO}$) mice were

generated by crossing Pdia1$^{fl/fl}$ mice [21] with VE–Cadherin (Cdh5)–Cre mice [22] on a C57BL/6 J background and used at 8–12 weeks.

Antibodies

Anti-PDIA1 (BD Bioscience, #610946, 1:1000), PDI Monoclonal Antibody RL90 (#MA3-019, 1:200) p-VEGFR2(1175) (Cell Signaling (CS), #3770, 1:1000), anti-VEGFR2 (CS#2479, 1:1000), anti-p-ERK1/2 (CS#9101, 1:1000), anti-ERK1/2 (CS#9102, 1:1000), anti-p-cSrc (CS#2101 1:1000), anti-cSrc (Santa Cruz # 5266, 1:1000), anti-PTP1B (D-4) (Santa Cruz, #133259, 1:1000), anti-Actin (Santa Cruz, #47778, 1:1000), anti-Rab5 (Santa Cruz #46692, 1:200), anti-Rab7 (B-3) (Santa Cruz# 376362, 1:200), anti CD31 (BD Biosciences# 550274, 1:200), anti-IsolectinB4 (Vector #B-1205, 1:200), anti-Flag (Sigma, #F7425, 1:1000) were used. Secondary antibodies, Goat Anti-Rabbit IgG–HRP conjugate (Bio Rad, #170-6515, 1:2000), Goat Anti-mouse IgG–HRP conjugate (Bio Rad, #170-6516, 1:2000), Alexa Fluor 568 goat anti Rat IgG (Invitrogen, # A-11077, 1:1000), Alexa Fluor 488 goat anti mouse IgG (Invitrogen, # A11001, 1:1000), Alexa Fluor-488-goat anti rabbit IgG (Invitrogen, #A11008), Alexa Fluor-546-goat anti mouse IgG (Invitrogen, #A11003), Alexa Fluor-546-goat anti rabbit IgG (Invitrogen, #A11010), Alexa Fluor-488-goat anti mouse IgG (Invitrogen, #A11001)were used.

siRNA and adenoviruses

siPDIA1 sense 5′-UGAGUCUUGAUUUCACCUC-3′, anti-sense 5′-GAGGUGAAA UCAAGACUCA-3′ [20]. Adenovirus expressing shNox4 (Ad.shNox4) and Ad.mitochondria-targeted catalase (Ad.Mito-catalase) [9] as well as Ad.flag-hPDIA1WT and the Ad.flag-hPDIA1–CS (C53S, C56S, C397S, C400S; inactive mutant) [18] were previously described.

Mouse retinal angiogenesis model

Eyes from postnatal day 5 (p5) mice were enucleated and fixed in 4% paraformaldehyde for 30 min. Retinas were dissected and permeabilized overnight in PBS containing 1% BSA and 0.5% Triton X-100. The permeabilized retinas were incubated with biotin-conjugated isolectinB4 (IB4) (20 μg/ml, Sigma-Aldrich), followed by Alexa Fluor 488-conjugated streptavidin (Invitrogen Life Technologies). After washes, samples were flat-mounted using Vectashield (Vector Labs) mounting medium and imaged under a fluorescence microscope. The total length, number of branch points and tip cells of IB4-positive vessels in the retina were quantified by two independent investigators in a blind fashion on composite high-magnification images using Image J software (v 1 0.52).

Aortic ring sprouting assay

Aortic ring sprouting assay was performed as described previously [23]. Isolated aorta from WT and Pdia1$^{+/-}$ mice at 8–12 weeks was cut into 5 mm rings. In some experiments, the aorta rings from WT mice were infected with lentivirus (lenti-scramble shRNA (shCont) *vs* lenti-shPdia1) in OpTi–MEM for 24 h. The aortic rings were embedded on Matrigel on 48 well plate with 2.5% FBS–OpTi–MEM, and then monitored for 5–7 days with changing media every other day. Mice in each group were $n = 5$ and number of aortic rings from one

mouse averaged 10 (the total number of aortic rings averaged 50). Numbers of sprouting branches from ECs were counted and normalized to control shRNA or WT mice.

Mouse hind limb ischemia model

Mice at 8–12 weeks were subjected to unilateral hindlimb surgery under anesthesia with intraperitoneal administration of ketamine (87 mg/kg) and xylazine (13 mg/kg) as we reported [24–26]. Briefly, the left femoral artery was exposed, ligated both proximally and distally using 6–0 silk sutures and the vessels between the ligatures were excised. We measured ischemic (left)/nonischemic (right) limb blood flow ratio using a laser Doppler blood flow (LDBF) analyzer (PeriScan PIM 3 System; Perimed).

Bone marrow transplantation (BMT)

BMT of mice at 8–12 weeks was performed as we previously reported [18, 24]. BM cells were isolated by density gradient separation. Recipient mice were lethally irradiated with 9.5 Gy and received an intravenous injection of 3 million donor BM cells 24 h after irradiation. As reported before transplantation efficiency has been validated [24]. Hindlimb ischemia was induced at 6–8 weeks after BMT.

Matrigel plug assay in vivo

500 μL Growth factor reduced Matrigel (Corning, REF353097) containing VEGF (50 ng/mL), bFGF (100 ng/mL), heparin (60 unit) was injected subcutaneously in mice and then harvested for analysis after 3 days.

Histology and immunohistochemistry

Mice were sacrificed, and ischemic and non-ischemic gastrocnemius skeletal muscles at day 7 or 14 after hindlimb ischemia were harvested, fixed with 4% PFA overnight at 4 °C, and followed by sucrose dehydration and optimal cutting temperature (OCT) embedding [18, 24, 27]. The 7 μm thick sections were stained with anti-mouse CD31 antibody (for capillary density) or anti-PDIA1 antibody, followed by biotinylated anti-mouse IgG antibody (Vector Laboratories) as described previously [27]. For immunohistochemistry, we used Vectorstain Elite (Vector Laboratories) followed by DAB (3,3′-diaminobenzidine tetrahydrochloride) (Vector Laboratories). Immunofluorescence analysis was performed at day 7 after ischemia with primary anti-CD31 antibody for overnight at 4 °C, followed by anti-PDIA1 antibody for 30 min at room temperature (RT). Then, the secondary antibodies (Alexa Fluor 568 goat anti Rat IgG or Alexa Fluor 488 goat anti mouse IgG) were incubated for 15 min at RT. In each experiment, DAPI (Invitrogen) was used for nuclear counter-staining. We used Mouse On Mouse (MOM) kit (Vector lab, BMK-2202) to avoid non-specific antibody binding. Images were taken using a fluorescence microscope (Keyence, BZ-X700) or an Axioscope microscope with a 20 objective. Microscopy images were acquired with axiovision 4.8.2 software, BZ-X Analyzer software and ZEN 2.3 software (Zeiss).

For IsolectinB4 staining for Matrigel plug assay, mice were sacrificed at 3 days after Matrigel plug, and solid Matrigel plug were harvested and fixed by overnight 4% PFA incubation and followed by 70% ethanol and embedded in paraffin. To determine the capillary density, Matrigel sections were stained with anti-mouse isolectin B4 antibody

(BD Biosciences) followed by biotinylated anti-mouse IgG antibody (Vector Laboratories) as described previously [28]. Images were captured by Axio scope microscope (Zeiss) and processed by AxioVision 4.8 (Zeiss).

Cell culture

The primary pool HUVECs (human Umbilical Vein Endothelial Cells) were purchased from the Lonza (CC-2519, USA). The cells were cultured in the recommended medium (Endo-Gro) supplemented with 5% fetal bovine serum (Life Technologies, Gaithersburg, MD, USA), 50 units/ml penicillin (Life Technologies), and 50 μg/ml streptomycin (Life Technologies). HUVECs were used until passages 6 for all experiments.

Transfection

For siRNA transfection, HUVECs were transfected with siR-NAs (30 nM) for scrambled siControl (Ambione) or PDIA1 (Sigma) with Oigofectamine (Invitrogen, 12252011) for 3 h. Then the medium was changed to complete media and incubated for 48 h at 37 °C before experiments. For adenovirus transfection, HUVECs were transfected with adenoviruses for 1 h and then the medium was changed to complete media, and incubated for 24 h at 37 °C before experiments.

Modified Boyden chamber migration assay

Modified Boyden Chamber assays were conducted in duplicate 24-well transwell chambers [18, 24, 29]. The upper insert (8-μm pores coated with 0.1% gelatin) containing serum starved HUVEC suspensions (6×10^4 cells) were placed in the bottom 24-well chamber containing fresh media with 0.2% FBS and stimulants. The chamber was incubated at 37 °C for 6 h. The upper insert membrane was fixed with 4% PFA for 10 min and stained with crystal violet. Cells remaining on the top of the transwells were removed with cotton swabs and migrated cells were imaged at six random fields (× 200 magnifications) and counted as described previously [30].

Cell proliferation (BrdU incorporation) assay

HUVECs (100,000 cells) were plated on coverslips in 0.5% FBS EndoGro for 24 h to synchronize cells, followed by incubation with 5 μM Bromodeoxyuridine (BrdU) with or without VEGF (20 ng/mL) for 24 h. The BrdU incorporation were detected using In Situ Cell Proliferation kit, FLUOS (Roche) with minor modification [31]. The cells were photographed with fluorescence microscope (Keyence, BZ-X700) using × 40 objective. The percentage of BrdU-labelled cells was determined by counting > 400 nuclei per samples as BrdU-positive/total nuclei.

Spheroid sprouting assay

HUVECs were trypsinized and counted, and then 4×10^4 cells were adjusted to a volume of 10 ml in 5% EndoGro with 0.25% CMC (CarboxylMethylCellulose, Sigma C4888). 100 μl of the cell suspension was applied into each well of a 96-well plate with Poly-HEMA (Poly[2-hydroxyethylmethacrylate], Sigma P3932) coated U-bottoms and incubated at 37 °C for 1 day. For sprouting assay, a 24-well plate was prepared by adding 1 ml PBS to

each cavity that will not be used for a spheroid gel and pre-warmed the plate at 37 °C. The spheroids from 96-well plate were harvested using a Pasteur pipet and transferred into a 50 ml Falcon tube, and then centrifuge for 3 min at 200× g. The supernatant was carefully removed and the spheroids were overlaid with the 0.8% CMC containing 20% FBS with 1 × M199 (we used 500 μl for 50 spheroids). Collagen solution (Collagen Type1 Rat tail 3.81 mg/ml, Corning 354236) with ratio of 1:1 (v/v) was added rapidly and carefully mixed the solution containing the spheroids. 900 μl of the spheroid solution was added per cavity of 24 well plate was incubated at 37°C for 45 min. 100 μl of EndoGro with or without VEGF (20 ng/mL) was added on top of the gels and incubated with the spheroid gels at 37 °C for 24 h. Then the gels were fixed and photographed. The spheroid sprouting tube length and number of branches were measured using Image J1.53C (Java 1.8.0-172, 64 bit) software.

Western blot analysis and immunoprecipitation

Cells were lysed in buffer [50 mM HEPES (pH 7.4), 5 mM EDTA, 100 mM NaCl, 1% Triton X-100, protease inhibitors (10 μg/ml aprotinin, 1 mmol/L phenylmethyl-sulfonyl fluoride, 10 μg/ml leupeptin) and phosphatase inhibitors (50 mmol/L sodium fluoride, 1 mmol/L sodium orthovanadate, 10 mmol/L sodium pyrophosphate)]. Lysates with or without immunoprecipitation were used for Western blotting, as we reported [18, 24, 29, 30]. Western blot acquisition was performed using a ImageQuant TL 8.1 software.

DCP–Bio1 assay to detect CysOH-formed (sulfenylated) proteins

To measure sulfenic acid (CysOH) formation (sulfenylation) of proteins, cells were lysed in degassed-specific lysis buffer [50 mM HEPES, pH7.0 at room temperature, 5 mM EDTA, 50 mM NaCl, 50 mM NaF, 1 mM Na_3VO_4, 10 mM sodium pyrophosphate, 5 mM Iodoacetamide (IAA), 100 μM DTPA, 1% Triton-X-100, protease inhibitor, 200 unit/mL catalase (Calbiochem), 200 μM DCP–Bio1 (KaraFast, USA)] and then DCP–Bio1-bound proteins were pulled down with streptavidin beads (Thermo scientific, USA) for overnight at 4 °C. DCP–Bio1 conjugated sulfenylated-proteins were determined by immunoblotting with specific antibodies, as reported [13, 18, 30].

ROS measurement—To detect intracellular ROS, HUVECs stimulated with VEGF were incubated with 10 μM CM–H_2DCFDA [5-(and 6)-chloromethyl-2′,7′-dichlorodihydrofluorescein diacetate, acetyl ester, Invitrogen] for 6 min at 37 °C, fixed with 4% paraformaldehyde for 10 min at room temperature, and then mounted with VECTASHIELD Mounting Medium with DAPI. DCF fluorescence was measured by confocal microscopy (Zeiss) using the identical setting and the same exposure condition in each experiment. Relative DCF fluorescence with DAPI positive cells were analyzed using Image J (NIH). We confirmed that DCF fluorescence was abolished by incubation with adeno-catalase suggesting that DCF signal mainly detects intracellular H_2O_2, as we reported [30]. In some experiments to detect cellular redox status, we also used cell-permeant fluorescence indicator, CellROX Orange (Invitrogen). Cells were incubated with 5 μM CellROX for 30 min and fluorescence images were taken using confocal microscopy, as previously described with minor modifications [32].

Immunofluorescence

For cultured cells, HUVECs on glass coverslips were rinsed quickly in ice-cold PBS, fixed with freshly prepared 4% paraformaldehyde in PBS for 10 min at room temperature, permeabilized in 0.05% Triton X-100 in PBS for 5 min, and rinsed sequentially in PBS, 50 μmol/L NH_4Cl and PBS for 10 min each. After incubation for 1 h in blocking buffer (PBS + 3%BSA), cells were incubated with primary antibody for overnight at 4 °C, washed three times with PBS, and then incubated in Alexa Fluor 488 or 647-conjugated IgG for 1 h at room temperature, and cells rinsed with PBS. Cells on coverslips were mounted onto glass slides using Vectashield (Vector Laboratories) and images were taken by confocal microscopy.

Statistics analysis

Data are presented as mean ± SEM. Each experiment was performed a minimum of three to make sure similar results are reproducible. We performed blinded to group allocation during data collection and analysis. Data were compared between groups of cells and animals by unpaired two tailed Student *t* test when one comparison was performed or by ANOVA for multiple comparisons. When significance was indicated by ANOVA, the Tukey post-hoc and Bonferroni multiple comparison analysis was used to specify between group differences. Values of $*p < 0.05$, $**p < 0.01$, $***p < 0.001$ were considered statically significant. Statistical tests were performed using Graph pad Prism v8 (GraphPad Software, San Diego, CA).

Results

PDIA1 is required for postnatal angiogenesis in vivo

To address the role for endogenous PDIA1 in postnatal developmental angiogenesis, we used a retinal angiogenesis model in mice carrying a single Pdia1 allele ($Pdia1^{+/-}$). Of note, global Pdia1 (*P4HB*) knockout (KO) mice are embryonic lethal [17]. $Pdia1^{+/-}$ retina (P5) stained with isolectin B4 showed a significant decrease in the number of branching points in the vascular plexus (top and middle) and tip cells in the vascular front (bottom) without affecting either migration of the vascular plexus towards the periphery (length) or the percentage of vascular retinal area to total retinal area, as compared to wild type (WT, littermate control $Pdia1^{+/+}$) retina (Fig. 1a). These results suggest that Pdia1 is required for postnatal developmental angiogenesis in vivo. We also performed the Matrigel plug assay and found that $Pdia1^{+/-}$ mice showed a significant reduction in isolectin-B4 staining in Matrigel as compared to WT mice (Fig. 1b). To verify the role of PDIA1 in angiogenic processes without contribution of systemic factors, such as blood flow, blood pressure and homeostatic regulation, we further performed an aortic ring sprouting ex vivo angiogenesis assay. As shown in (Fig. 1c), the number of branching sprouts from the edge of aortic segments was significantly reduced in $Pdia1^{+/-}$ mice as compared to WT mice. These results suggest that PDIA1 is required for postnatal angiogenesis in vivo and ex vivo.

Endothelial PDIA1 is required for post-ischemic angiogenesis in vivo

To address the role of PDIA1 in reparative angiogenesis in vivo, we used a mouse hindlimb ischemia (HLI) model, an animal model of Peripheral Artery Disease (PAD), which induces ischemia by femoral artery ligation and excision [24, 33]. Immunohistochemistry (Fig. 2a), western blot (Fig. 2b) and immunofluorescence (Fig. 2c) analysis reveal that PDIA1 protein expression was increased and colocalized with $CD31^+$ ECs in ischemic muscles at day 7 after hindlimb ischemia. These results suggest that Pdia1 is upregulated in $CD31^+$ ECs during reparative angiogenesis. Since $Pdia1^{+/-}$ mice had no significant difference in ischemia-induced limb perfusion recovery, as compared to WT mice (Supplemental Fig. 1a, b), we performed bone marrow transplantation (BMT) to eliminate contribution of BM cells. The lethally irradiated $Pdia1^{+/-}$ mice reconstituted with WT–BM showed significant reduction of blood flow recovery and $CD31^+$ capillary density in ischemic muscles, as compared to control group (WT mice reconstituted with WT–BM) (Supplemental Fig. 1c, d). These results suggest the haploinsufficiency of PDIA1 in non-hematopoietic cells, including ECs, in reparative neovascularization after hindlimb ischemia. To demonstrate the role of endothelial Pdia1 in post-ischemic angiogenesis in vivo, we generated EC-specific Pdia1 conditional knockout ($Pdia1^{ECKO}$) mice by crossing $Pdia1^{fl/fl}$ mice with mice expressing Cre recombinase under control of the VE-cadherin promoter (Cdh5–Cre). We found that perfusion recovery (Fig. 2d) and angiogenesis ($CD31^+$ capillaries) (Fig. 2e) in response to hindlimb ischemia were significantly impaired in $Pdia1^{ECKO}$ mice as compared to WT mice. These data suggest that endothelial PDIA1 plays a critical role in ischemia-induced reparative angiogenesis in vivo.

PDIA1 is required for VEGF-induced signaling and angiogenesis in ECs

We next examined the role of PDIA1 in VEGF-induced angiogenic responses, including EC migration, EC proliferation and capillary formation in primary cultured ECs. PDIA1 knockdown using specific siRNA in HUVECs almost completely inhibited VEGF-induced EC migration as measured by a modified Boyden chamber assay (Fig. 3a) as well as EC proliferation as measured by a BrdU incorporation assay (Fig. 3b). Using a Spheroid sprouting assay, we found that PDIA1 depletion significantly reduced the number of sprouting from spheroid of ECs with or without VEGF stimulation (Fig. 3c). To address the underlying mechanism, we examined the role of PDIA1 in VEGF signaling in ECs. PDIA1 siRNA significantly inhibited VEGF-induced phosphorylation of VEGFR2 (VEGFR2–pY1175) and its downstream p-ERK1/2 and p-Src without affecting the expression of the total protein (Fig. 3d). These results suggest that PDIA1 regulates VEGFR2 signaling to induce angiogenic responses in ECs.

To address mechanisms by which PDIA1 regulates VEGFR2 signaling, we examined the interactions between PDIA1 and VEGFR2. Co-immunoprecipitation assays showed that PDIA1 slightly bound to VEGFR2 in the basal state, which was further enhanced after VEGF stimulation within 5 min and their interactions remained for at least 30 min (Fig. 4a). To determine the subcellular localization of PDIA1 and VEGFR2, we performed immunofluorescence colocalization analysis using confocal microscopy. In the basal state, VEGFR2 was found at plasma membrane and perinucleus, where it partially co-localized with PDIA1 (Fig. 4b1). Their perinuclear colocalization was further enhanced after VEGF

stimulation for 5 min at the Rab5-positive early endosomes, where internalized VEGFR2 activates sustained angiogenic signaling [34], while their colocalization was less at the Rab7 + late endosome (Fig. 4b1). These results suggest that VEGF stimulation promotes PDIA1 binding to internalized VEGFR2 at early endosomes, thereby activating sustained VEGFR2 signalling in ECs.

VEGF induces sulfenylation of PDIA1 in a NOX4- and mitochondrial ROS-dependent manner in ECs

We previously reported that ROS, especially H_2O_2, derived from the NOX–mitoROS axis play an important role in VEGFR2 signaling and angiogenesis in ECs [9]. Since PDIA1 is shown to increase NOX activity in VSMC and macrophage [19], we examined the role of PDIA1 in VEGF-induced ROS production in ECs, as measured by DCF fluorescence which was abolished by Nox4 shRNA or catalase overexpression (Supplementary Fig. 2a), as we previously reported [9]. We found that PDIA1 knockdown with siRNA had no significant effect on VEGF-induced ROS production, as measured by DCF fluorescence (Fig. 5a) or CellROX orange (Supplementary Fig. 2c).

We next examined whether PDIA1 is a downstream target of VEGF-induced ROS to promote VEGFR2 signaling. It is shown that ROS induce oxidation of Cys residues in target proteins to form CysOH (sulfenylation) [10, 12, 13] and that PDIA1 has four redox active Cys residues (Cys53, Cys56, Cys397, and Cys400) in the catalytic domains [14–16, 35, 36]. Thus, we examined if VEGF induces sulfenylation of PDIA1 in ECs using a biotin-conjugated CysOH trapping probe, DCP–Bio1 [13]. We found that VEGF stimulation rapidly induced CysOH formation of PDIA1 within 5 min, peaking at 15 min, which gradually returned to the basal level within 2 h (Fig. 5b). Importantly, VEGF-induced PDIA1–CysOH formation was abolished by overexpression of Nox4 shRNA or mito-catalase (Fig. 5c) or “redox-dead” Cys oxidation-defective mutant PDIA1 in which the four active sites of Cys residues were mutated to Ser (PDIA1–CS) (Fig. 5d). We confirmed the significant reduction of Nox4 mRNA and VEGF-induced ROS production by Nox4 shRNA (Supplemental Fig. 2 a, b). These results suggest that VEGF induces sulfenylation of PDIA1 at redox active Cys residues in NOX4- and mitoROS-dependent manners in ECs.

Sulfenylation of PDIA1 promotes VEGFR2 signaling and angiogenesis

We next examined the functional significance of PDIA1 sulfenylation for VEGF-induced VEGFR2 signaling and angiogenic responses in ECs. Overexpression of Cys oxidation-defective PDIA1–CS mutant, but not PDIA1–WT, significantly inhibited VEGF-induced p-VEGFR2 at Tyr1175 as compared to control adenovirus (Ad.null) (Fig. 6a). Furthermore, PDIA1–CS overexpression significantly inhibited VEGF-induced VEGFR2 downstream signaling such as p-ERK1/2 or p-Src (Fig. 6b) as well as angiogenic responses such as EC migration (Fig. 6c) or EC proliferation (Fig. 6d), as compared to Ad.null (control). Of note, Ad.PDIA1–WT had no significant effects on VEGF-induced angiogenic responses (Supplemental Fig. 3a, b) and VEGFR2 signaling (Supplemental Fig. 3c) compared to Ad.null, suggesting that PDIA1–CS functions as a dominant negative in these responses.

To determine the mechanism by which PDIA1 sulfenylation promotes VEGFR2 phosphorylation, we examined the relationship between PDIA1 and protein tyrosine phosphatase 1B (PTP1B) which is shown to dephosphorylate p-VEGFR2 at Tyr1175 [37, 38] and is inactivated by Cys oxidation [30, 39, 40]. We first confirmed our previous observation that overexpression of PTP1B–WT inhibits VEGF-induced p-VEGFR2 at Tyr1175 (Fig. 7a). Importantly, VEGF stimulation promoted PDIA1 binding to PTP1B (Fig. 7b), which was associated with CysOH formation of PTP1B within 5 min (Fig. 7c). Of note, Cys oxidation-defective PDIA1–CS mutant overexpression inhibited VEGF-induced PTP1B sulfenylation (Fig. 7c) in addition to p-VEGFR2 (Fig. 6a). Thus, these results suggest that PDIA1 senses VEGF-induced ROS signal via sulfenylation, thereby promoting VEGFR2 signaling and angiogenesis via oxidative inactivation of PTP1B in ECs.

Discussion

We previously reported that “ROS-induced ROS release” orchestrated by NOX–mitoROS axis play an important role in VEGFR2 signaling and angiogenesis in ECs [9]; however, how highly diffusible ROS are sensed to activate VEGFR2 signaling is poorly understand. PDIA1 functions as an oxidoreductase depending on the redox environment. The role of endothelial PDIA1 in ROS-dependent VEGF signaling and angiogenesis as well as postnatal neovascularization in vivo was not previously reported. This study provides the first evidence that PDIA1 functions as a redox sensor that transmits VEGF-induced H_2O_2 signal via sulfenylation to promote VEGFR2 signaling and angiogenesis. Here we show that $Pdia1^{+/-}$ or PDIA1–ECKO mice exhibit impaired postnatal developmental and reparative angiogenesis in vivo. Mechanistically, VEGF stimulation in human ECs rapidly induced PDIA1–CysOH formation by NOX4–mitoROS axis, which in turn promotes endosomal VEGFR2 signaling via Cys oxidation of PTP1B that dephosphorylates p-VEGFR2, thereby driving angiogenesis (Fig. 8).

Since global PDIA1-deficient mice are embryonic lethal, we initially used $Pdia1^{+/-}$ heterozygous mice and found that PDIA1 plays an important role in postnatal angiogenesis using developmental retinal angiogenesis, Matrigel plug models and aortic ring spouting assays. The present study using EC-specific Pdia1 deficient mice with a hindlimb ischemia model suggests that PDIA1 is upregulated in angiogenic ECs in ischemic muscles and that endothelial Pdia1 has beneficial effects to restore perfusion recovery and promote reparative neovascularization in response to tissue ischemia. Consistent with our results, Tian et al. [41] reported that PDI is highly upregulated in hypoxic myocardial capillary ECs; however, its functional significance in myocardial infarction remains unknown. By contrast, previous studies using megakaryoyte-specific PDIA1-deficient mice show that platelet Pdia1 is involved in pathological effects such as laser injury-induced thrombus formation [21] and glycoprotein Ibα-mediated platelet–neutrophil interactions under thrombo-inflammatory conditions [42]. Thus, PDIA1 function may differ depending on cell types, redox environments, or disease types.

In vitro study shows that PDIA1 knockdown using specific siRNA in HUVECs significantly inhibited VEGF-induced angiogenic responses, including EC migration, EC proliferation, and capillary tube formation. Consistent with our results, Tian et al. [41] reported that loss

of PDI increased apoptosis, reduced migration and tube formation in ECs exposed to chronic hypoxia. It is shown that Endo-PDI (also termed ERp46) is required for TNFα-induced angiogenesis in HUVECs [43]. Although PDIA1 was reported to interact with NOX subunits such as p22phox and p47phox to increase NOX activity in VSMCs or macrophage [15, 19], PDIA1 depletion had no significant effect on VEGF-induced ROS production in HUVECs as measured by DCF–DA or CellROX. Thus, our findings suggest that PDIA1 plays an essential role in VEGF-induced angiogenic responses without affecting ROS production in ECs.

In quiescent ECs which are in a reduced state, we previously reported that reduced form of PDIA1 functions as a thiol reductase for mitochondrial fission protein Drp1 to keep it in reduced and inactive form to maintain normal mitochondrial and EC function [18]. Kang et al. [44] reported that antioxidant peroxiredoxin II (PrxII) knockdown in quiescent ECs increases H_2O_2 levels in basal state, which induces intramolecular disulfide bonds formation between Cys^{1199} and Cys^{1206} in the C-terminal tail of VEGFR2, resulting in VEGFR2 being inactive in caveolae, and thus no longer responded to VEGF stimulation. By contrast, our previous [8, 9] and present study demonstrated that VEGF-induced NOX4–mitoROS signal axis promotes VEGFR2 activation and reparative angiogenesis by sulfenylation of PDIA1. These findings suggest that role of ROS in the basal and VEGF-stimulated ECs is different, such that elevation of ROS in the basal state is inhibitory, while VEGF-induced ROS is stimulatory for VEGFR2 activation. Thus, keeping VEGFR2 in the reduced form in quiescent ECs by PrxII is required for VEGFR2 activation by VEGF-induced ROS.

Signaling function of ROS is in part mediated through sulfenylation of Cys residues in target proteins [10, 12, 13]. The present study using CysOH trapping probe (DCP–Bio1) [13], Nox4 shRNA or overexpression of mito-catalase revealed that VEGF stimulation in quiescent ECs rapidly induced sulfenylation (Cys oxidation) of PDIA1 via the Nox4–mitoROS axis, which promotes VEGFR2 activation in endosomes and reparative angiogenesis. These findings are consistent with the notion that oxidative environment with increased ROS production converts the reduced form of PDI to the oxidized form of PDI which functions as a thiol oxidase for its target proteins [15]. Using “redox-dead” PDIA1 inactive mutant in which four reactive Cys residues (Cys53, Cys56, Cys397, and Cys400) in the two a/a’ (CGHC) redox active motifs [14–16, 35, 36] were mutated to Ser (PDIA1–C/S mutant), we showed that PDIA1–CysOH formation plays an important role in VEGFR2 signaling and angiogenic responses in ECs. Consistent with our finding, Kenche et al. reported that sulfenylated PDI is increased as a protective adaptation to cigarette smoke exposure in the murine model of chronic obstructive pulmonary disease [45]. Our results suggest that PDIA1 functions as a redox sensor that transmits VEGF-induced Nox4–mitoROS signaling via sulfenylation at Cys resides in the redox active sites, which drives VEGFR2 signaling and angiogenesis in ECs. Zhou et al. reported that C-terminal CGHC redox-active sites of PDIA1 is involved in platelet function and coagulation in vivo [21]. Although PDIA1 has other Cys residues (Cys310, Cys342), they do not possess low pKa values, raising the possibility that these Cys residues might not be direct targets of VEGF-induced ROS. Future studies are required to identify active site Cys residues responsible for PDIA1 CysOH formation and to determine whether other post-translational modification

of PDIA1, such as S-gluthathionylation [46] and S-nitrosylation [47], plays a role in VEGF-induced angiogenesis.

The important question is how VEGF-induced NOX4–mitoROS axis contributes to PDIA1–CysOH formation, resulting in promoting VEGFR2 phosphorylation. Although PDIA1 is mainly localized in the ER, but it is also in the cytosol [48–50], mitochondria [51], or cell surface [52]. It is shown that ligand binding to VEGFR2 induces VEGFR2 dimerization and subsequent internalization to Rab5 + endosomes which provide specific intracellular compartments required for assembly of signaling complexes to activate VEGFR2/PLCγ/ERK signaling [6, 7]. The present study shows that PDIA1 is sulfenylated and colocalizes with endocytosed VEGFR2 at Rab5 + early endosomes after VEGF stimulation. It is reported that endosomes structurally contact with ER [53] and that ER also forms membrane contact sites with mitochondria, termed mitochondria-associated membrane (MAM) [54]. Thus, PDIA1 may associate with internalized VEGFR2 at the ER–endosome contact sites to achieve compartmentalized redox relay from mitoROS to PDIA1–CysOH axis to drive sustained endosomal VEGFR2 signaling.

PTP1B is shown to dephosphorylate VEGFR2 when VEGFR2-containing early endosomes become positioned in close proximity to the ER [37]. Of note, PTP1B is anchored to the ER surface by a C-terminal 35-amino acid hydrophobic domain with its catalytic domain exposed to the cytoplasm and is inactivated by Cys oxidation [5, 55, 56]. Our studies show that overexpression of “redox dead” PDIA1–CS mutant which inhibits PDIA1 sulfenylation prevents VEGF-induced Cys oxidation of PTP1B and VEGFR2 phosphorylation. Thus, PDIA1 transmits VEGF-induced H_2O_2 signal to PTP1B, which leads to PTP1B sulfenylation and subsequent inactivation. This in turn increases VEGFR2 phosphorylation in the early endosomes which are in close proximity to the ER, thereby promoting sustained VEGFR2 signaling and angiogenesis. Taken together, it is likely that VEGF-induced redox signaling mediated through the mitoROS/PDIA1-CysOH/PTP1B–CysOH/VEGFR2 axis may take place at the “redox triangle” formed by mitochondria, ER and early endosomes.

In summary, we demonstrate that endothelial PDIA1 plays an important role in ROS-dependent VEGFR2 signaling and angiogenesis in ECs as well as postnatal developmental and reparative angiogenesis in vivo. Findings of this study will advance the understanding of the molecular mechanisms by which VEGF-induced ROS-induced ROS release (NOX–mitoROS relay) is sensed at the specific intracellular compartments to drive VEGFR2 signaling and productive angiogenesis. Our results suggest that PDIA1 functions as a redox sensor that transmits VEGF-induced NOX–mitoROS signal via CysOH formation to promote VEGFR2 signaling and angiogenesis via oxidation of PTP1B that dephosphorylates VEGFR2. Furthermore, the present study provides new insights into oxidized PDIA1 as a potential therapeutic target for treatment of ROS- and angiogenesis-dependent cardiovascular diseases.

Supplementary Material

Refer to Web version on PubMed Central for supplementary material.

Acknowledgements

We would like to thank Dr. Henar Cyuervo Grajal at University of Illinois at Chicago for assisting retinal angiogenesis in initial study.

Funding

This work was supported by National Institute of Health grants: R01HL160014, R01HL135584 (to M.U.-F.), R01HL147550 (to M.U.-F., T.F), R01HL133613, R01HL116976 (to T.F., M.U.-F.), R01HL070187 (to T.F.), R01EY011766, R01EY030500, R21EY032265 (R.B.C.), Veterans Administration Merit Review Award 2I01BX001232 (to T.F.), 101BX001233 (R.B.C.), R01HL118526 (D.W.E.). The VA Career Scientist Award (IK6BX005228) (to R.B.C.). R.B. Caldwell is the recipient of a Research Career Scientist Award from the Department of Veterans Affairs. The contents do not represent the views of the Department of Veterans Affairs or the United States Government. The funders had no role in study design, data collection and analysis, decision to publish, or preparation of the manuscript.

Data availability

The authors declare that all supporting data are available within the article (and its data supplement).

References

1. Ushio-Fukai M (2006) Redox signaling in angiogenesis: role of NADPH oxidase. Cardiovasc Res 71(2):226–235. 10.1016/j.cardiores.2006.04.015 [PubMed: 16781692]
2. Ushio-Fukai M (2007) VEGF signaling through NADPH oxidase-derived ROS. Antioxid Redox Signal 9(6):731–739. 10.1089/ars.2007.1556 [PubMed: 17511588]
3. Ushio-Fukai M, Urao N (2009) Novel role of NADPH oxidase in angiogenesis and stem/progenitor cell function. Antioxid Redox Signal 11(10):2517–2533. 10.1089/ARS.2009.2582 [PubMed: 19309262]
4. Fukai T, Ushio-Fukai M (2011) Superoxide dismutases: role in redox signaling, vascular function, and diseases. Antioxid Redox Signal 15(6):1583–1606. 10.1089/ars.2011.3999 [PubMed: 21473702]
5. Lee SR, Kwon KS, Kim SR, Rhee SG (1998) Reversible inactivation of protein-tyrosine phosphatase 1B in A431 cells stimulated with epidermal growth factor. J Biol Chem 273(25):15366–15372. 10.1074/jbc.273.25.15366 [PubMed: 9624118]
6. Simons M (2012) An inside view: VEGF receptor trafficking and signaling. Physiology (Bethesda) 27(4):213–222. 10.1152/physiol.00016.2012 [PubMed: 22875452]
7. Eichmann A, Simons M (2012) VEGF signaling inside vascular endothelial cells and beyond. Curr Opin Cell Biol 24(2):188–193. 10.1016/jxeb.2012.02.002 [PubMed: 22366328]
8. Fukai T, Ushio-Fukai M (2020) Cross-talk between NADPH oxidase and mitochondria: role in ROS signaling and angiogenesis. Cells. 10.3390/cells9081849
9. Kim YM, Kim SJ, Tatsunami R, Yamamura H, Fukai T, Ushio-Fukai M (2017) ROS-induced ROS release orchestrated by Nox4, Nox2, and mitochondria in VEGF signaling and angiogenesis. Am J Physiol Cell Physiol 312(6):C749–C764. 10.1152/ajpcell.00346.2016 [PubMed: 28424170]
10. Poole LB, Karplus PA, Claiborne A (2004) Protein sulfenic acids in redox signaling. Annu Rev Pharmacol Toxicol 44:325–347. 10.1146/annurev.pharmtox.44.101802.121735 [PubMed: 14744249]
11. Ushio-Fukai M (2006) Localizing NADPH oxidase-derived ROS. Sci STKE. 10.1126/stke.3492006re8
12. Charles RL, Schroder E, May G, Free P, Gaffney PR, Wait R, Begum S, Heads RJ, Eaton P (2007) Protein sulfenation as a redox sensor: proteomics studies using a novel biotinylated dimedone analogue. Mol Cell Proteomics 6(9):1473–1484. 10.1074/mcp.M700065-MCP200 [PubMed: 17569890]

13. Poole LB, Nelson KJ (2008) Discovering mechanisms of signaling-mediated cysteine oxidation. Curr Opin Chem Biol 12(1):18–24. 10.1016/jxbpa.2008.01.021 [PubMed: 18282483]
14. Benham AM (2012) The protein disulfide isomerase family: key players in health and disease. Antioxid Redox Signal 16(8):781–789. 10.1089/ars.2011.4439 [PubMed: 22142258]
15. Laurindo FR, Pescatore LA, Fernandes Dde C (2012) Protein disulfide isomerase in redox cell signaling and homeostasis. Free Radical Biol Med 52(9):1954–1969. 10.1016/j.freeradbiomed.2012.02.037 [PubMed: 22401853]
16. Cremers CM, Jakob U (2013) Oxidant sensing by reversible disulfide bond formation. J Biol Chem 288(37):26489–26496. 10.1074/jbc.R113.462929 [PubMed: 23861395]
17. Xiong B, Jha V, Min JK, Cho J (2020) Protein disulfide isomerase in cardiovascular disease. Exp Mol Med 52(3):390–399. 10.1038/s12276-020-0401-5 [PubMed: 32203104]
18. Kim YM, Youn SW, Sudhahar V, Das A, Chandhri R, Cuervo Grajal H, Kweon J, Leanhart S, He L, Toth PT, Kitajewski J, Rehman J, Yoon Y, Cho J, Fukai T, Ushio-Fukai M (2018) Redox regulation of mitochondrial fission protein Drp1 by protein disulfide isomerase limits endothelial senescence. Cell Rep 23(12):3565–3578. 10.1016/j.celrep.2018.05.054 [PubMed: 29924999]
19. Laurindo FR, Fernandes DC, Amanso AM, Lopes LR, Santos CX (2008) Novel role of protein disulfide isomerase in the regulation of NADPH oxidase activity: pathophysiological implications in vascular diseases. Antioxid Redox Signal 10(6):1101–1113. 10.1089/ars.2007.2011 [PubMed: 18373437]
20. Hahm E, Li J, Kim K, Huh S, Rogelj S, Cho J (2013) Extracellular protein disulfide isomerase regulates ligand-binding activity of alphaMbeta2 integrin and neutrophil recruitment during vascular inflammation. Blood 121(19):3789–3800. 10.1182/blood-2012-11-467985 [PubMed: 23460613]
21. Zhou J, Wu Y, Wang L, Rauova L, Hayes VM, Poncz M, Essex DW (2015) The C-terminal CGHC motif of protein disulfide isomerase supports thrombosis. J Clin Invest 125(12):4391–4406. 10.1172/JCI80319 [PubMed: 26529254]
22. Chen MJ, Yokomizo T, Zeigler BM, Dzierzak E, Speck NA (2009) Runx1 is required for the endothelial to haematopoietic cell transition but not thereafter. Nature 457(7231):887–891. 10.1038/nature07619 [PubMed: 19129762]
23. Baker M, Robinson SD, Lechertier T, Barber PR, Tavora B, D'Amico G, Jones DT, Vojnovic B, Hodivala-Dilke K (2011) Use of the mouse aortic ring assay to study angiogenesis. Nat Protoc 7(1):89–104. 10.1038/nprot.2011.435 [PubMed: 22193302]
24. Chen GF, Sudhahar V, Youn SW, Das A, Cho J, Kamiya T, Urao N, McKinney RD, Surenkhuu B, Hamakubo T, Iwanari H, Li S, Christman JW, Shantikumar S, Angelini GD, Emanueli C, Ushio-Fukai M, Fukai T (2015) Copper transport protein antioxidant-1 promotes inflammatory neovascularization via chaperone and transcription factor function. Sci Rep 5:14780. 10.1038/srep14780 [PubMed: 26437801]
25. Tojo T, Ushio-Fukai M, Yamaoka-Tojo M, Ikeda S, Patrushev N, Alexander RW (2005) Role of gp91phox (Nox2)-containing NAD(P)H oxidase in angiogenesis in response to hindlimb ischemia. Circulation 111(18):2347–2355. 10.1161/01.CIR.0000164261.62586.14 [PubMed: 15867174]
26. Urao N, Sudhahar V, Kim SJ, Chen GF, McKinney RD, Kojda G, Fukai T, Ushio-Fukai M (2013) Critical role of endothelial hydrogen peroxide in post-ischemic neovascularization. PLoS ONE 8(3):e57618. 10.1371/journal.pone.0057618 [PubMed: 23472092]
27. Das A, Sudhahar V, Chen GF, Kim HW, Youn SW, Finney L, Vogt S, Yang J, Kweon J, Surenkhuu B, Ushio-Fukai M, Fukai T (2016) Endothelial antioxidant-1: a key mediator of copper-dependent wound healing in vivo. Sci Rep 6:33783. 10.1038/srep33783 [PubMed: 27666810]
28. Chabot S, Jabrane-Ferrat N, Bigot K, Tabiasco J, Provost A, Golzio M, Noman MZ, Giustiniani J, Bellard E, Brayer S, Aguerre-Girr M, Meggetto F, Giuriato S, Malecaze F, Galiacy S, Jais JP, Chose O, Kadouche J, Chouaib S, Teissie J, Abitbol M, Bensussan A, Le Bouteiller P (2011) A novel antiangiogenic and vascular normalization therapy targeted against human CD160 receptor. J Exp Med 208(5):973–986. 10.1084/jem.20100810 [PubMed: 21482699]
29. Oshikawa J, Kim SJ, Furuta E, Caliceti C, Chen GF, McKinney RD, Kuhr F, Levitan I, Fukai T, Ushio-Fukai M (2012) Novel role of p66Shc in ROS-dependent VEGF signaling and

angiogenesis in endothelial cells. Am J Physiol Heart Circ Physiol 302(3):H724–732. 10.1152/ajpheart.00739.2011 [PubMed: 22101521]

30. Oshikawa J, Urao N, Kim HW, Kaplan N, Razvi M, McKinney R, Poole LB, Fukai T, Ushio-Fukai M (2010) Extracellular SOD-derived H2O2 promotes VEGF signaling in caveolae/lipid rafts and post-ischemic angiogenesis in mice. PLoS ONE 5(4):e10189. 10.1371/journal.pone.0010189 [PubMed: 20422004]
31. Wang S, Amato KR, Song W, Youngblood V, Lee K, Boothby M, Brantley-Sieders DM, Chen J (2015) Regulation of endothelial cell proliferation and vascular assembly through distinct mTORC2 signaling pathways. Mol Cell Biol 35(7):1299–1313. 10.1128/MCB.00306-14 [PubMed: 25582201]
32. Ash D, Sudhahar V, Youn SW, Okur MN, Das A, O'Bryan JP, McMenamin M, Hou Y, Kaplan JH, Fukai T, Ushio-Fukai M (2021) The P-type ATPase transporter ATP7A promotes angiogenesis by limiting autophagic degradation of VEGFR2. Nat Commun 12(1):3091. 10.1038/s41467-021-23408-1 [PubMed: 34035268]
33. Urao N, Inomata H, Razvi M, Kim HW, Wary K, McKinney R, Fukai T, Ushio-Fukai M (2008) Role of nox2-based NADPH oxidase in bone marrow and progenitor cell function involved in neovascularization induced by hindlimb ischemia. Circ Res 103(2):212–220. 10.1161/CIRCRESAHA.108.176230 [PubMed: 18583711]
34. Simons M, Gordon E, Claesson-Welsh L (2016) Mechanisms and regulation of endothelial VEGF receptor signalling. Nat Rev Mol Cell Biol 17(10):611–625. 10.1038/nrm.2016.87 [PubMed: 27461391]
35. Freedman RB, Gane PJ, Hawkins HC, Hlodan R, McLaughlin SH, Parry JW (1998) Experimental and theoretical analyses of the domain architecture of mammalian protein disulphide-isomerase. Biol Chem 379(3):321–328. 10.1515/bchm.1998.379.3.321 [PubMed: 9563828]
36. Alanen HI, Salo KE, Pekkala M, Siekkinen HM, Pirneskoski A, Ruddock LW (2003) Defining the domain boundaries of the human protein disulfide isomerases. Antioxid Redox Signal 5(4):367–374. 10.1089/152308603768295096 [PubMed: 13678523]
37. Nakamura Y, Patrushev N, Inomata H, Mehta D, Urao N, Kim HW, Razvi M, Kini V, Mahadev K, Goldstein BJ, McKinney R, Fukai T, Ushio-Fukai M (2008) Role of protein tyrosine phosphatase 1B in vascular endothelial growth factor signaling and cell-cell adhesions in endothelial cells. Circ Res 102(10):1182–1191. 10.1161/CIRCRESAHA.107.167080 [PubMed: 18451337]
38. Lanahan AA, Lech D, Dubrac A, Zhang J, Zhuang ZW, Eichmann A, Simons M (2014) PTP1b is a physiologic regulator of vascular endothelial growth factor signaling in endothelial cells. Circulation 130(11):902–909. 10.1161/CIRCULATIONAHA.114.009683 [PubMed: 24982127]
39. Salmeen A, Andersen JN, Myers MP, Meng TC, Hinks JA, Tonks NK, Barford D (2003) Redox regulation of protein tyrosine phosphatase 1B involves a sulphenyl-amide intermediate. Nature 423(6941):769–773. 10.1038/nature01680 [PubMed: 12802338]
40. Londhe AD, Bergeron A, Curley SM, Zhang F, Rivera KD, Kannan A, Coulis G, Rizvi SHM, Kim SJ, Pappin DJ, Tonks NK, Linhardt RJ, Boivin B (2020) Regulation of PTP1B activation through disruption of redox-complex formation. Nat Chem Biol 16(2):122–125. 10.1038/s41589-019-0433-0 [PubMed: 31873221]
41. Tian F, Zhou X, Wikstrom J, Karlsson H, Sjoland H, Gan LM, Boren J, Akyurek LM (2009) Protein disulfide isomerase increases in myocardial endothelial cells in mice exposed to chronic hypoxia: a stimulatory role in angiogenesis. Am J Physiol Heart Circ Physiol 297(3):H1078–1086. 10.1152/ajpheart.00937.2008 [PubMed: 19617410]
42. Li J, Kim K, Jeong SY, Chiu J, Xiong B, Petukhov PA, Dai X, Li X, Andrews RK, Du X, Hogg PJ, Cho J (2019) Platelet protein disulfide isomerase promotes glycoprotein ibalpha-mediated platelet-neutrophil interactions under thromboinflammatory conditions. Circulation 139(10):1300–1319. 10.1161/CIRCULATIONAHA.118.036323 [PubMed: 30586735]
43. Camargo LL, Babelova A, Mieth A, Weigert A, Mooz J, Rajalingam K, Heide H, Wittig I, Lopes LR, Brandes RP (2013) Endo-PDI is required for TNFalpha-induced angiogenesis. Free Radical Biol Med 65:1398–1407. 10.1016/j.freeradbiomed.2013.09.028 [PubMed: 24103565]
44. Kang DH, Lee DJ, Lee KW, Park YS, Lee JY, Lee SH, Koh YJ, Koh GY, Choi C, Yu DY, Kim J, Kang SW (2011) Peroxiredoxin II is an essential antioxidant enzyme that prevents the

oxidative inactivation of VEGF receptor-2 in vascular endothelial cells. Mol Cell 44(4):545–558. 10.1016/j.molcel.2011.08.040 [PubMed: 22099303]

45. Kenche H, Ye ZW, Vedagiri K, Richards DM, Gao XH, Tew KD, Townsend DM, Blumental-Perry A (2016) Adverse outcomes associated with cigarette smoke radicals related to damage to protein-disulfide isomerase. J Biol Chem 291(9):4763–4778. 10.1074/jbc.M115.712331 [PubMed: 26728460]
46. Townsend DM, Manevich Y, He L, Xiong Y, Bowers RR Jr, Hutchens S, Tew KD (2009) Nitrosative stress-induced s-glutathionylation of protein disulfide isomerase leads to activation of the unfolded protein response. Cancer Res 69(19):7626–7634. 10.1158/0008-5472.CAN-09-0493 [PubMed: 19773442]
47. Uehara T, Nakamura T, Yao D, Shi ZQ, Gu Z, Ma Y, Masliah E, Nomura Y, Lipton SA (2006) S-nitrosylated protein-disulphide isomerase links protein misfolding to neurodegeneration. Nature 441(7092):513–517. 10.1038/nature04782 [PubMed: 16724068]
48. Wroblewski VJ, Masnyk M, Khambatta SS, Becker GW (1992) Mechanisms involved in degradation of human insulin by cytosolic fractions of human, monkey, and rat liver. Diabetes 41(4):539–547. 10.2337/diab.41.4.539 [PubMed: 1607078]
49. Turano C, Coppari S, Altieri F, Ferraro A (2002) Proteins of the PDI family: unpredicted non-ER locations and functions. J Cell Physiol 193(2):154–163. 10.1002/jcp.10172 [PubMed: 12384992]
50. Parakh S, Atkin JD (2015) Novel roles for protein disulphide isomerase in disease states: a double edged sword? Front Cell Dev Biol 3:30. 10.3389/fcell.2015.00030 [PubMed: 26052512]
51. El Hindy M, Hezwani M, Corry D, Hull J, El Amraoui F, Harris M, Lee C, Forshaw T, Wilson A, Mansbridge A, Hassler M, Patel VB, Kehoe PG, Love S, Conway ME (2014) The branched-chain aminotransferase proteins: novel redox chaperones for protein disulfide isomerase–implications in Alzheimer's disease. Antioxid Redox Signal 20(16):2497–2513. 10.1089/ars.2012.4869 [PubMed: 24094038]
52. Soares Moretti AI, Martins Laurindo FR (2017) Protein disulfide isomerases: redox connections in and out of the endoplasmic reticulum. Arch Biochem Biophys 617:106–119. 10.1016/j.abb.2016.11.007 [PubMed: 27889386]
53. Raiborg C, Wenzel EM, Stenmark H (2015) ER-endosome contact sites: molecular compositions and functions. EMBO J 34(14):1848–1858. 10.15252/embj.201591481 [PubMed: 26041457]
54. Aoyama-Ishiwatari S, Hirabayashi Y (2021) Endoplasmic reticulum-mitochondria contact sites-emerging intracellular signaling hubs. Front Cell Dev Biol 9:653828. 10.3389/fcell.2021.653828 [PubMed: 34095118]
55. Boivin B, Yang M, Tonks NK (2010) Targeting the reversibly oxidized protein tyrosine phosphatase superfamily. Sci Signal. 10.1126/scisignal.3137pl2
56. Frangioni JV, Beahm PH, Shifrin V, Jost CA, Neel BG (1992) The nontransmembrane tyrosine phosphatase PTP-1B localizes to the endoplasmic reticulum via its 35 amino acid C-terminal sequence. Cell 68(3):545–560. 10.1016/0092-8674(92)90190-n [PubMed: 1739967]

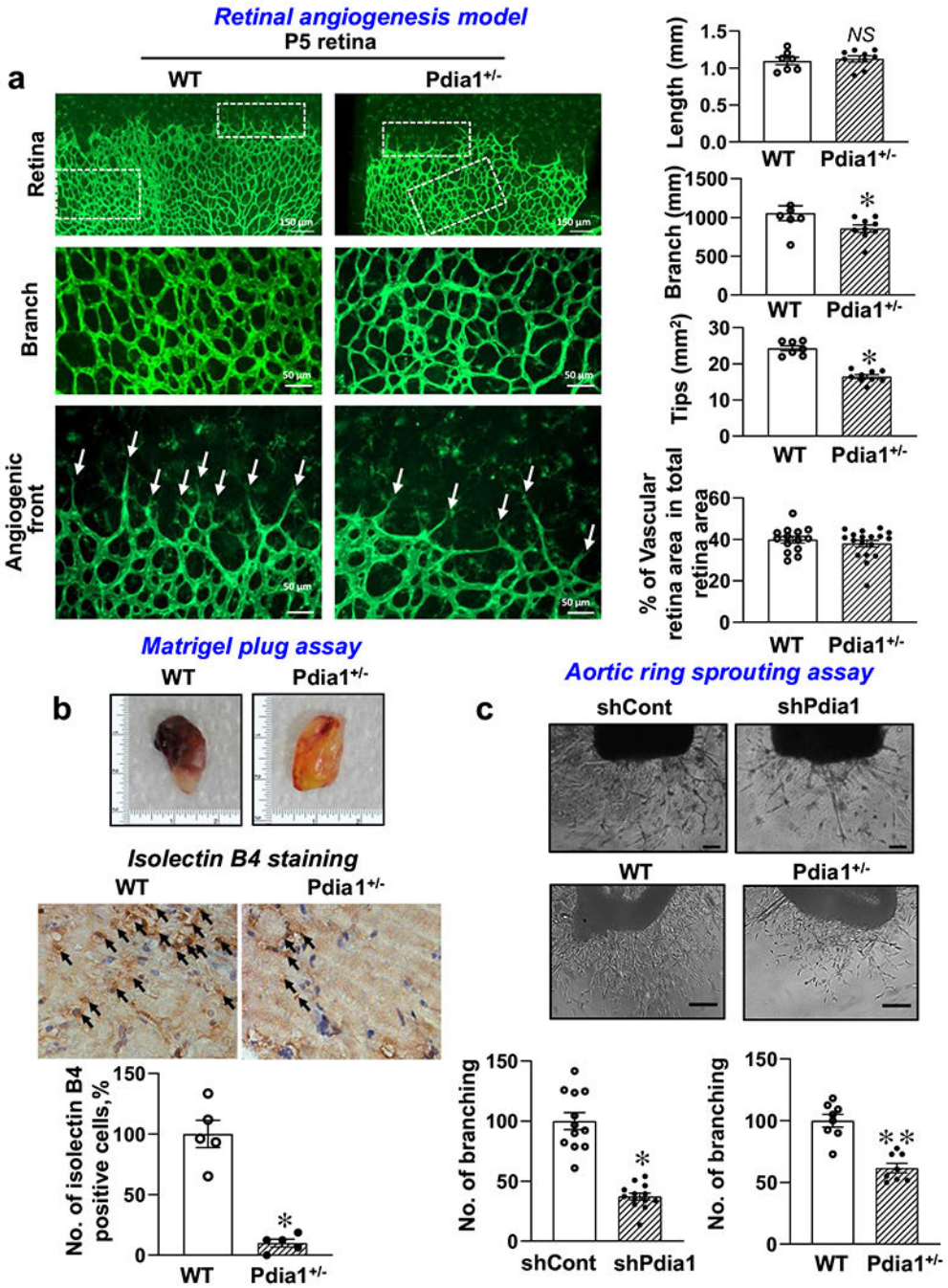

Fig. 1.

PDIA1 is required for postnatal angiogenesis in vivo. (**a**) Retinal whole-mount staining with Isolectin B4 (IB4) antibody of P5 pups from WT ($n = 7$) or Pdia1$^{+/-}$ ($n = 9$) mice. Arrowheads show tip cell sprouting and filopodia. The images show whole retina structure, remodeling plexus (branching points), and angiogenic fronts (tip cells). The quantitative results show retina length from center, number of branching points, and number of tip cells and the percentage of vascular retinal area to total retinal area. Results were presented as mean ± SEM. *$p < 0.05$. (**b**) Growth factor-reduced Matrigel containing VEGF (50 ng/mL),

bFGF (100 ng/mF), heparin (60 unit) was injected subcutaneously in WT ($n = 4$) or Pdia1$^{+/-}$ ($n = 4$) mice and then harvested for analysis after 3 days. The neovascularization in Matrigel was determined by staining with isolectin-B4 antibody. The images were representative from 3 to 4 mice and presented as mean ± SEM. *$p < 0.05$, vs WT. (**c**) Aortic ring sprouting assay was monitored on Matrigel for 5–7 days [upper panel; lenti-scramble shRNA (shCont) *vs* lenti-shPdia1 RNA. Lower panel; WT mice ($n = 3$–4) *vs* Pdia1$^{+/-}$ mice ($n = 3$–4)]. Numbers of sprouting branch from endothelial cells were counted and normalized by control shRNA or WT mice. The images were representative from at least three different experiments or different mice and presented as mean ± SEM. *$p < 0.05$, **$p < 0.01$ vs control or WT. ns, not significant

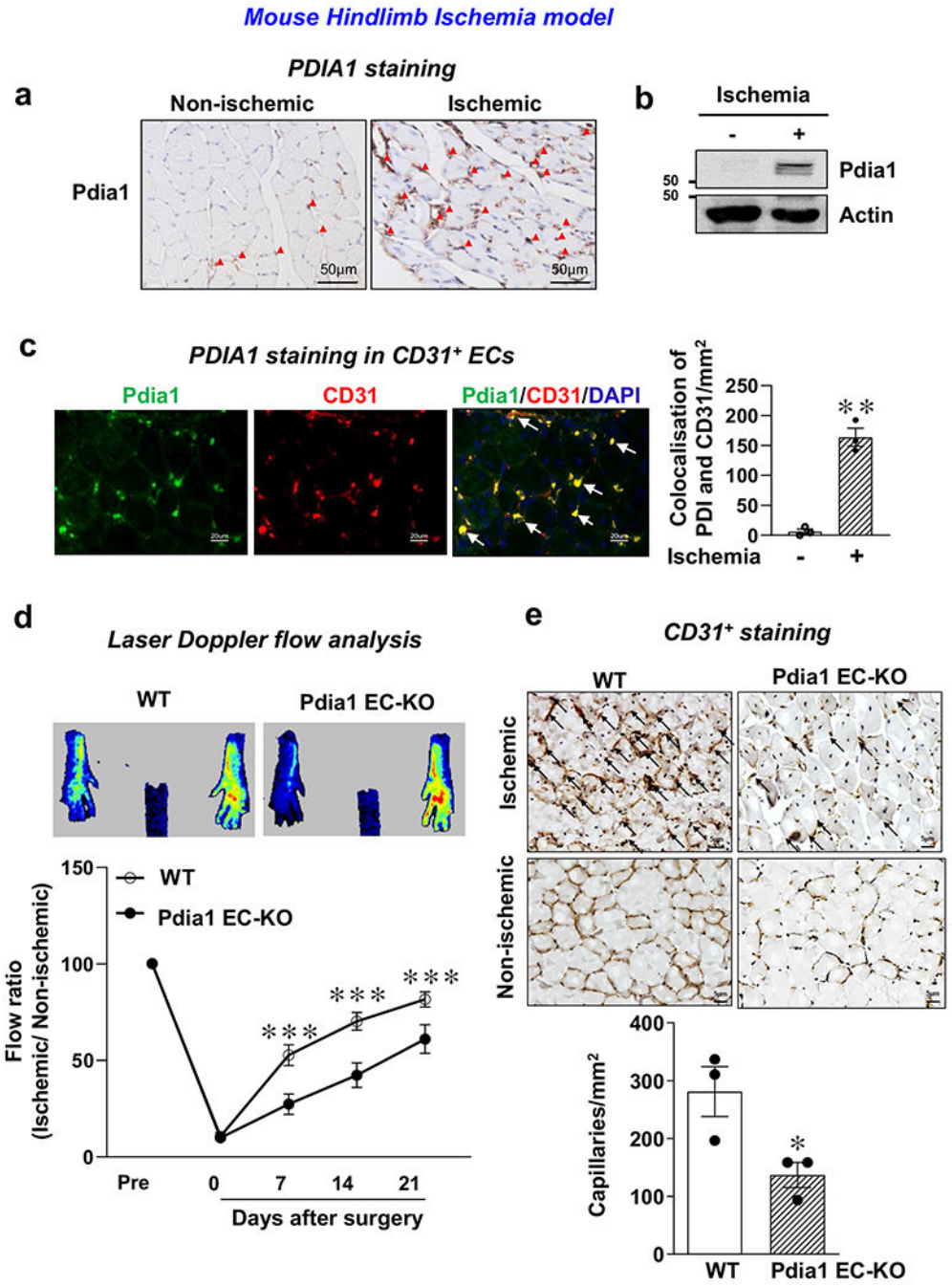

Fig. 2.

Endothelial PDIA1 is required for postnatal reparative angiogenesis in vivo. a and b, PDIA1 expression in ischemic and non-ischemic muscles at day 14 post-surgery by showing immunohisto-chemical analysis (**a**) and immunoblotting (**b**). (**c**) CD31 (red, EC marker) or PDIA1 (green) staining or their colocalization (merged, white arrows) in ischemic and non-ischemic gastrocnemius muscles at day 7 post-surgery. Scale bars, 20 μm. Bar graph represents CD31–PDIA1 co-localized cell numbers per field ($n = 3$, $^{**}p < 0.01$). (**d**) Blood flow recovery as determined by the ratio of foot perfusion between ischemic (left) and

ischemic (right) legs after hindlimb ischemia in WT and Pdia1^{ECKO} mice (n = 5). Upper panels show representative laser Doppler flow images showing limb perfusion recovery (red arrows show ischemic foot) at day 28 after ischemia in WT and Pdia1^{ECKO} mice, (**e**) Capillary density (CD31 staining) in ischemic and non-ischemic muscles of WT and Pdia1^{ECKO} mice at day 21. Scale bars, 5 μm. Bottom panels show their quantitative analysis (number of capillaries per mm square). Data are mean ± SEM (n = 6). *p < 0.05, ****p** < 0.01, *****p** < 0.001

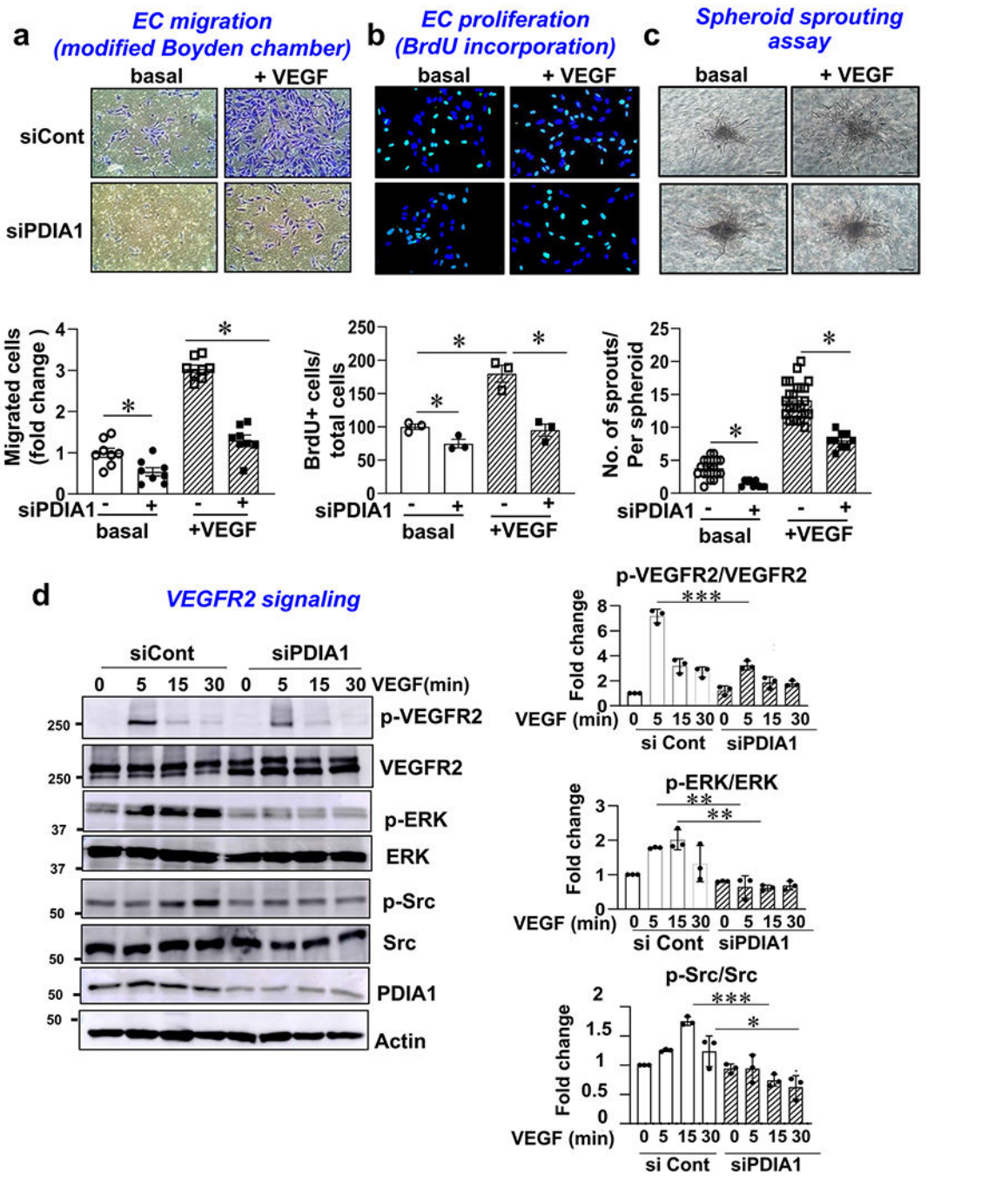

Fig. 3.

PDIA1 is required for VEGF-induced signaling and angiogenesis in ECs. HUVECs transfected with control or PDIA1 siRNAs were stimulated with VEGF (20 ng/ml) for 6 h were and then used for EC migration as measured by modified Boyden chamber assay ($n = 3$) (**a**), EC proliferation as measured by BrdU assay ($n = 3$) (**b**), and Spheroid sprouting assay ($n = 3–4$) (**c**). (**d**) HUVECs transfected with control or PDIA1 siRNAs were stimulated with VEGF (20 ng/ml) for indicated time. Lysates were immunoblotted (IB) with antibodies indicated. Actin is loading control. Graph represents the averaged fold change

over the basal control. Statistics analysis was performed by comparing two groups at each timepoint. ($n = 3$). *$p < 0.05$, **$p < 0.01$, ***$p < 0.001$

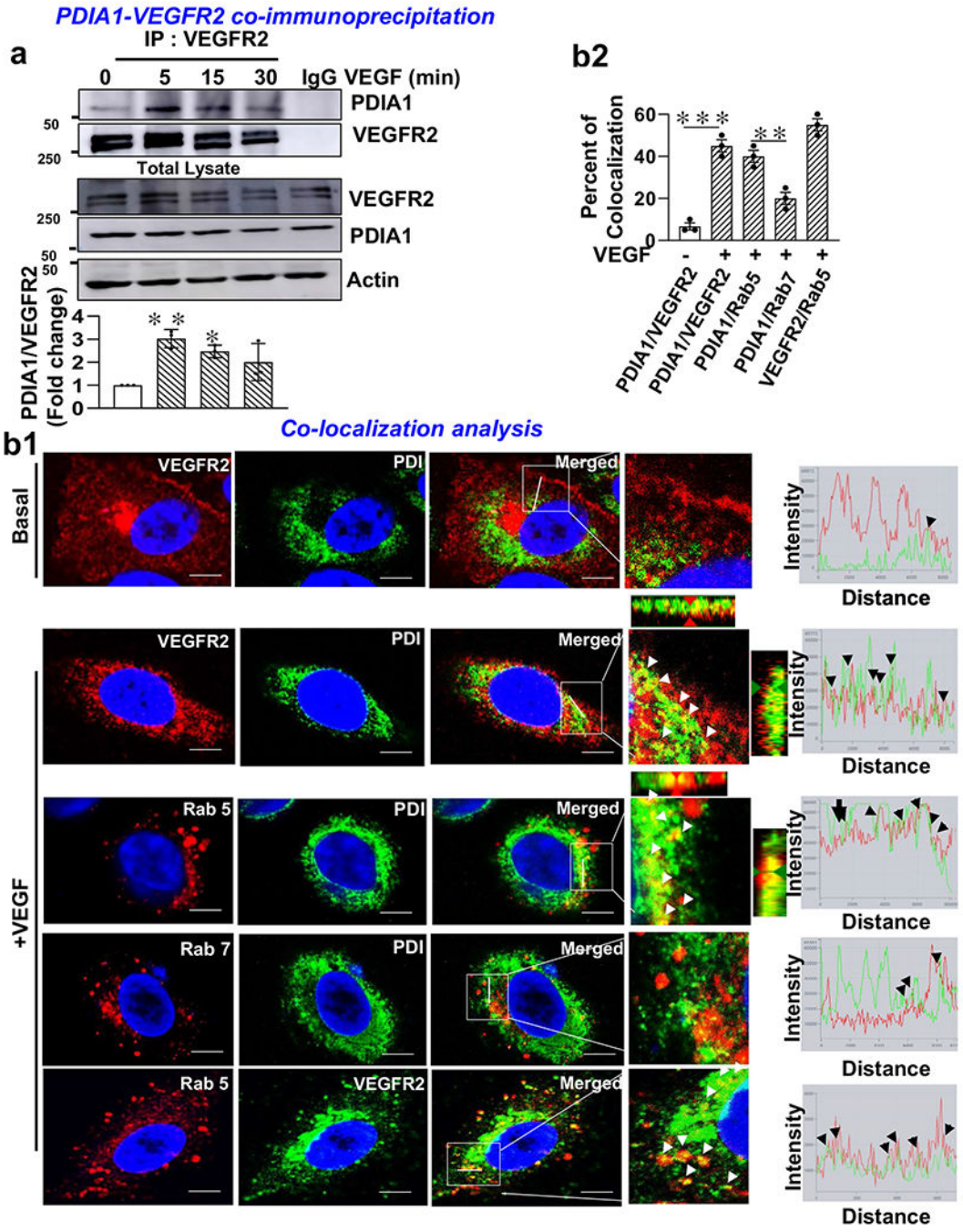

Fig. 4.

VEGF stimulation promotes PDIA1 binding to internalized VEGFR2 at early endosomes. (**a**) HUVECs stimulated with VEGF (20 ng/ml) were immunoprecipitated (IP) with VEGFR2 antibody or IgG (negative control), followed by IB with antibodies indicated. Lower panel represents the averaged fold change of PDIA1/VEGFR2 ratio over the basal ratio ($n = 3$, $*p < 0.05$, $**p < 0.01$). (**b**) HUVECs stimulated with or without VEGF for 5 min and co-stained for PDIA1 with VEGFR2 or early endosome markers (Rab5) or late endosome marker (Rab7). Images were taken using confocal microscopy. Yellow

fluorescence (white arrowheads) in merged images shows their co-localization (white box), which was analyzed by comparing the fluorescence intensity for each protein on white line in enlarged images (**b1**). Scale bars, 5μm. Bar graph represents the percentage of their co-localization (**b2**). Data are mean ± SEM ($n = 6$). *$p < 0.05$, **$p < 0.01$, ***$p < 0.001$

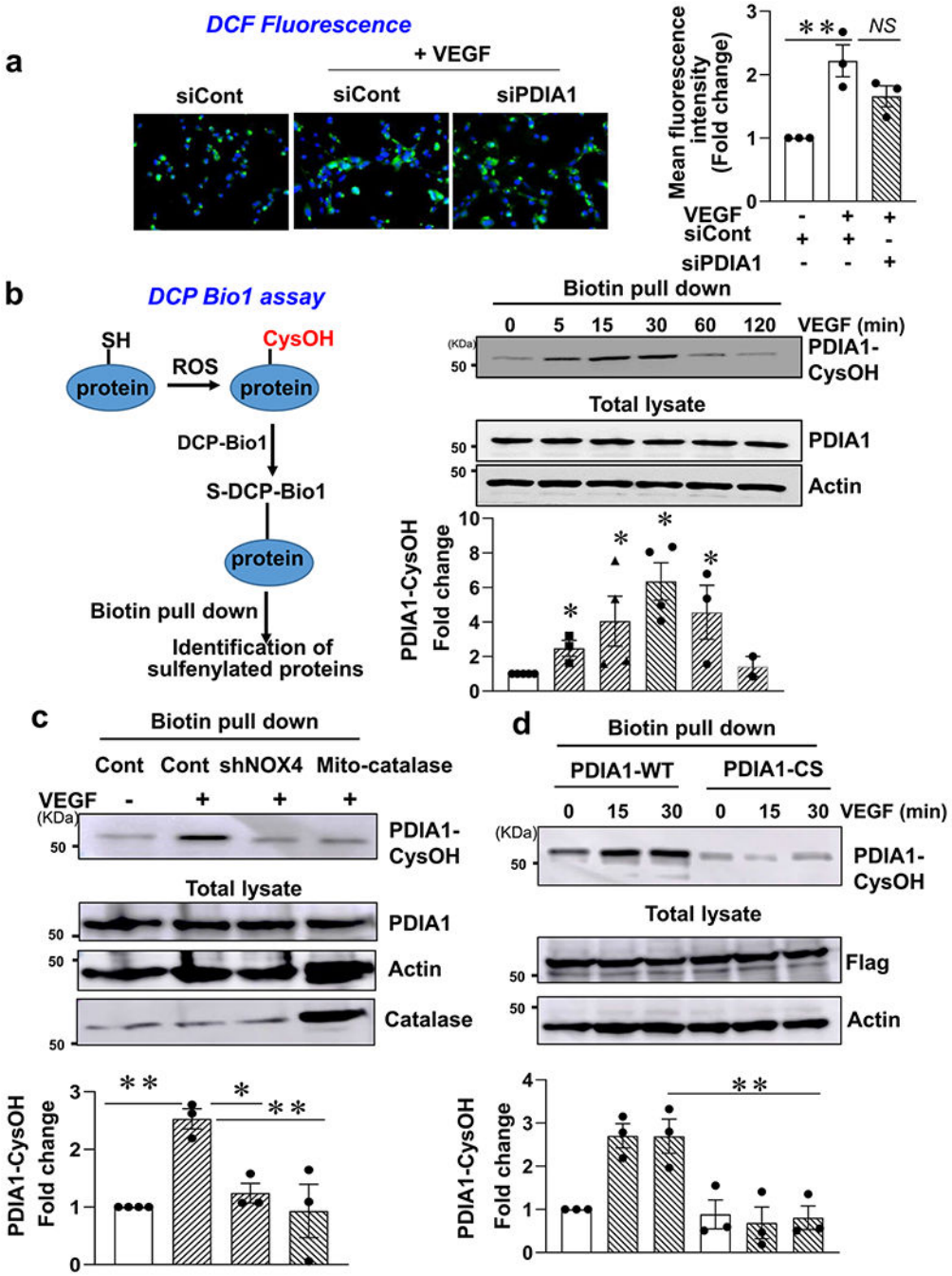

Fig. 5.

VEGF induces sulfenylation of PDIA1 in a NOX4- and mitochondrial ROS-dependent manner in ECs. (**a**) HUVECs transfected with control or PDIA1 siRNAs stimulated with or without VEGF (20 ng/ml) for 5 min were used to measure dichlorofluorescein (DCF) fluorescence and DAPI staining (blue). Bottom panel represents the averaged fold change of fluorescence intensity over the basal control ($n = 3$). (**b**–**d**) DCP–Bio1 assay to detect PDIA1 sulfenylation (CysOH formation). Scheme of DCP–Bio1 assay to detect of sulfenylated protein (**b**, left panel). HUVECs were stimulated with VEGF for indicated time (**b**, right

panel) or infected with Ad.null (cont), Ad.shNox4, or Ad.Mito-catalase (**c**), or Ad.flag–hPDIA1–WT or Ad.flag–hPDIA1–CS (redox-dead mutant) (**d**) and then stimulated with VEGF for 30 min. DCP–Bio1-labeled lysates were pulled down with streptavidin beads and then immunoblotted (IB) with anti-PDIA1 antibody to measure PDIA1–CysOH formation. Total lysates were IB with antibodies indicated. Data are mean ± SEM ($n = 3$). *$p < 0.05$, **$p < 0.01$

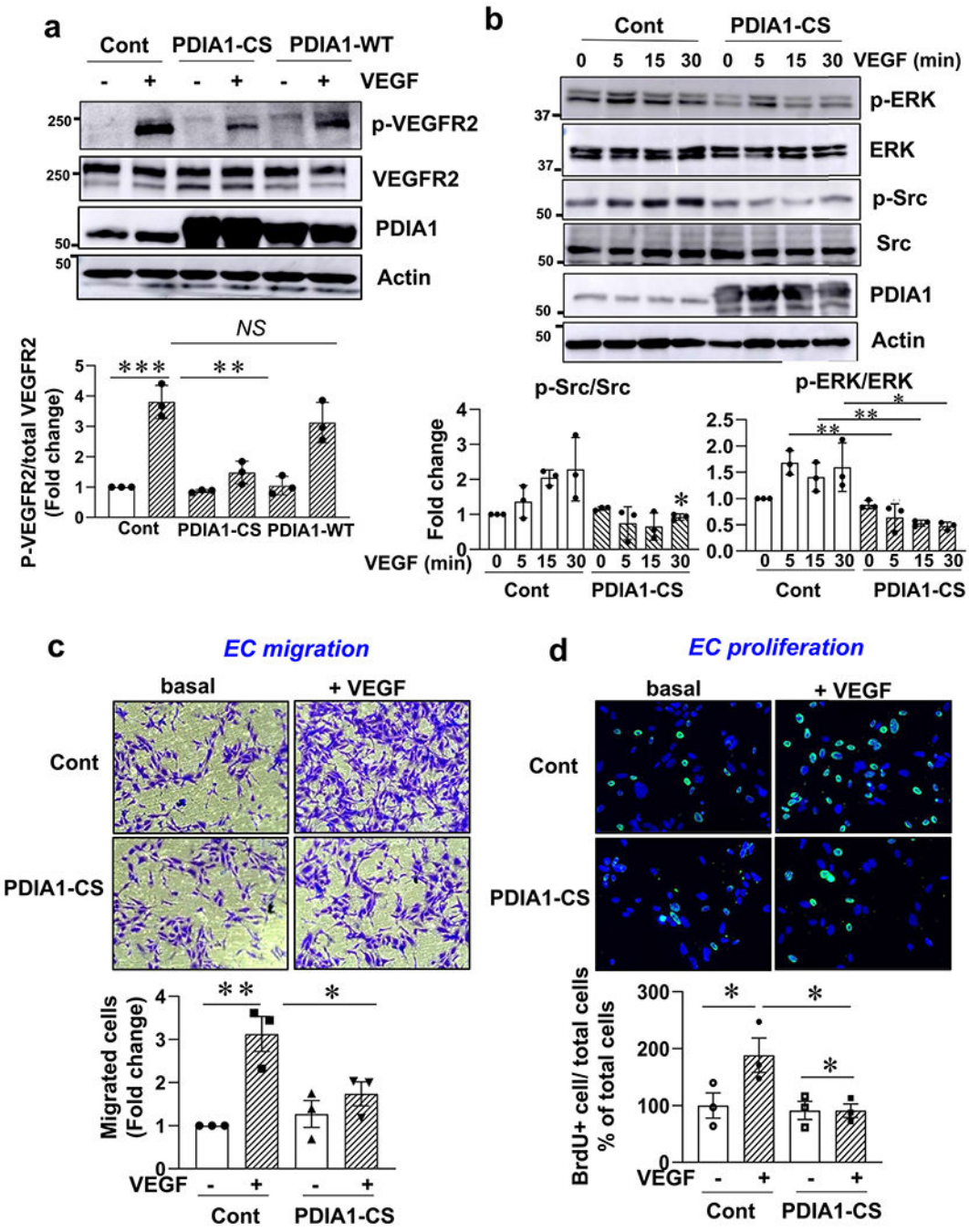

Fig. 6.

Sulfenylation of PDIA1 promotes VEGFR2 signaling and angiogenesis. (**a**, **b**, **c**, **d**) HUVECs were infected with Ad.null (Cont), Ad.PDIA1–WT or flag-hPDIA1–C/S (redox-dead mutant). Cells were stimulated with or without VEGF (20 ng/ml) for 5 min (**a**) or indicated times (**b**), and then lysates were IB with antibodies indicated (**a** and **b**). In (**b**), statistics analysis was performed by comparing two groups at each timepoint. In parallel, cells were used to measure EC migration with and without VEGF for 6 h, as measured by the modified Boyden chamber assay (**c**), and EC proliferation with and without VEGF for 24

h, as measured by BrdU assay (**d**). Data are mean ± SEM ($n = 3$). *$p < 0.05$, **$p < 0.01$, ***$p < 0.001$

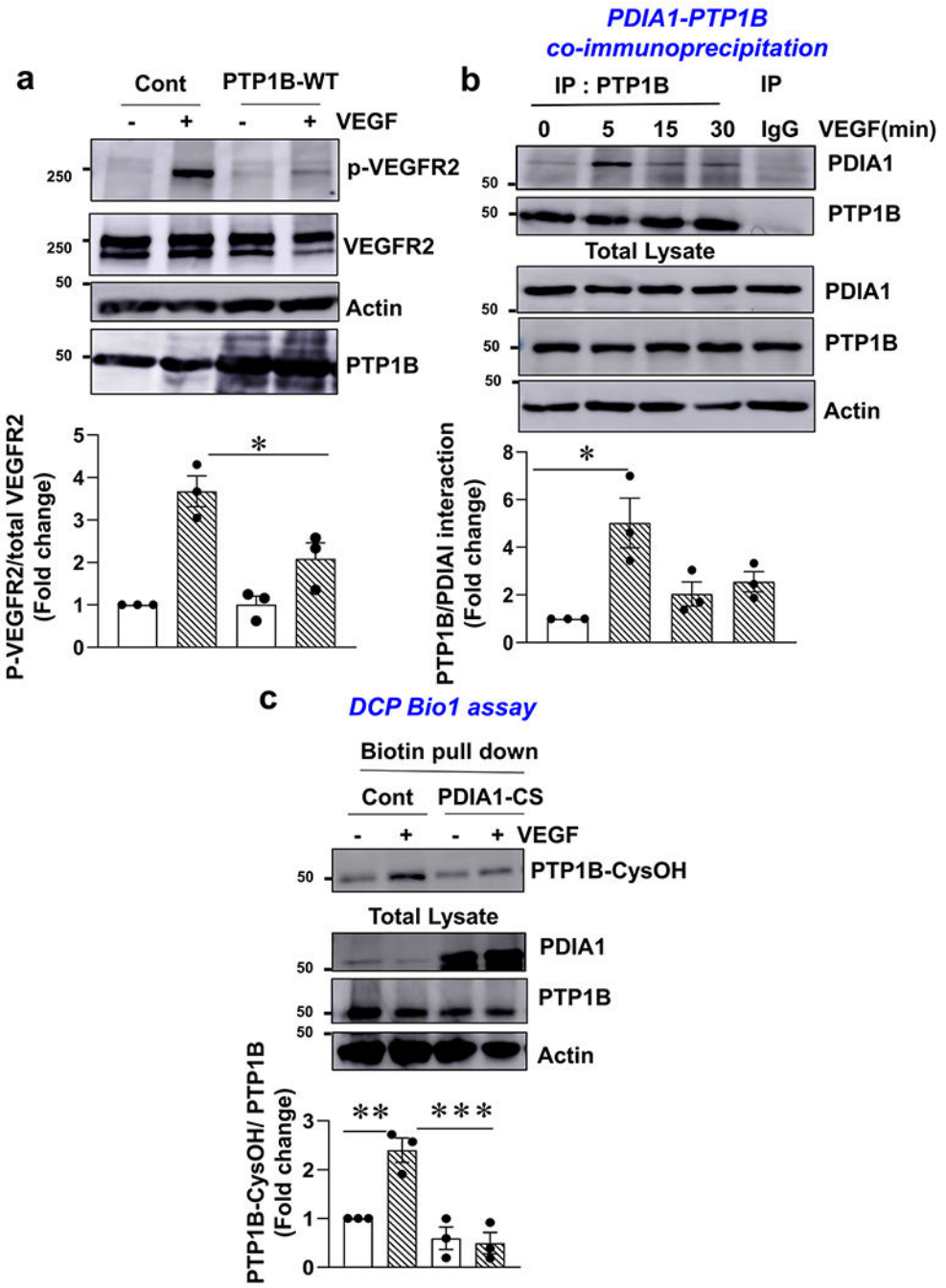

Fig. 7.

PDIA1–CysOH promotes VEGFR2 signaling via oxidative inactivation of PTP1B. (**a**) HUVECs infected with Ad.null (Cont) or Ad.PTP1B–WT were stimulated with or without VEGF (20 ng/ml) for 5 min, and then lysates were immunoblotted with anti-p-VEGFR2 (Y1175) or antibodies indicated. (**b**) HUVECs stimulated with VEGF for indicated times were immunoprecipitated (IP) with PTP1B antibody or IgG (negative control), followed by IB with antibodies indicated. Lower panel represents the averaged fold change of PTP1B/ PDIA1 ratio over the basal ratio ($n = 3$). (**c**) HUVECs infected with Ad.null or Ad. hPDIA1–

CS (redox-dead mutant) were stimulated with VEGF for 5 min. DCP–Bio1-labeled lysates were pulled down with streptavidin beads and then IB with anti-PTP1B antibody to measure PTP1B–CysOH formation. Total lysates were IB with antibodies indicated. Data are mean ± SEM (n = 3). *$p < 0.05$, **$p < 0.01$, ***$p < 0.001$

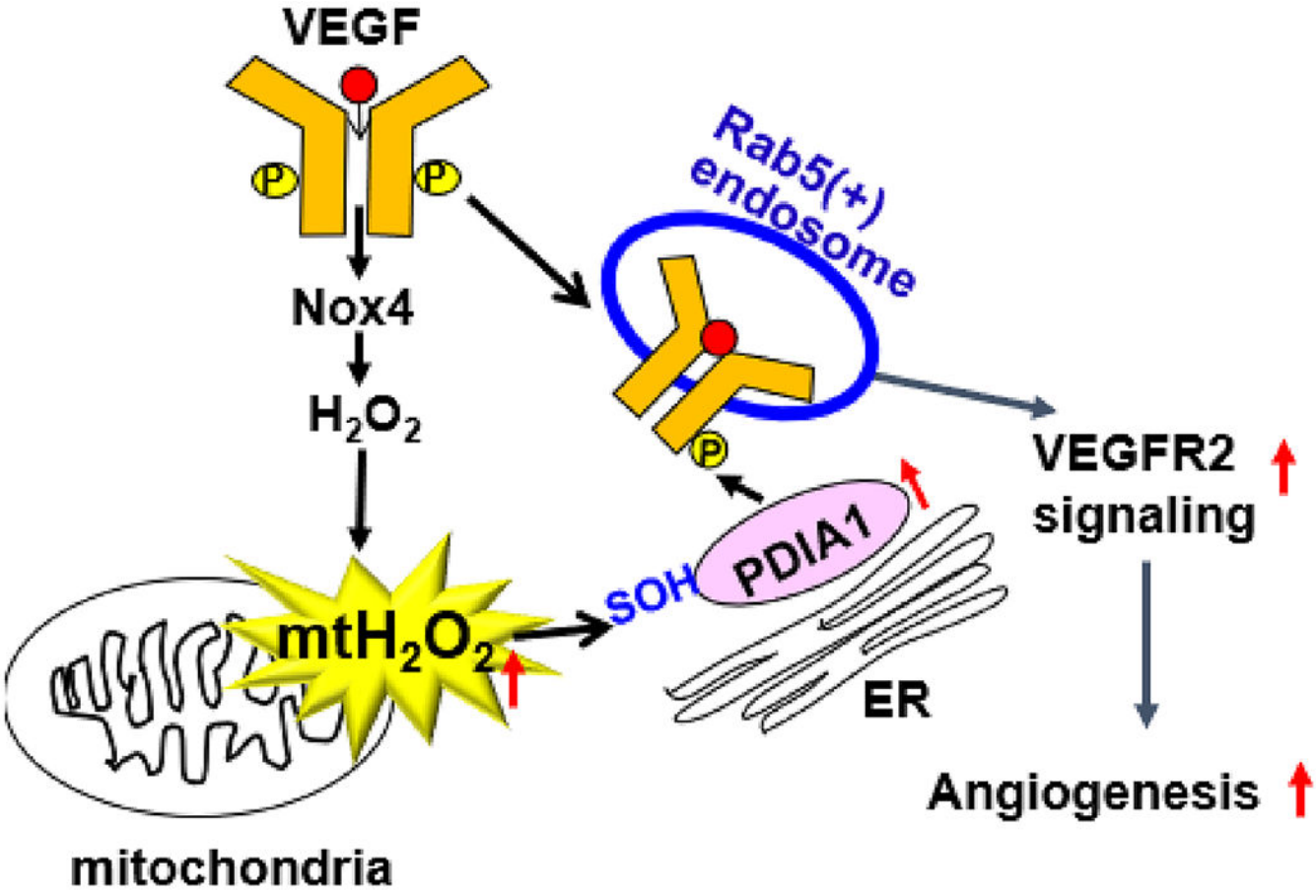

Fig. 8.

Proposed model. PDIA1 functions as a redox sensor that transmits VEGF-induced NOX–mitoROS signal via sulfenylation to promote VEGFR2 signaling and angiogenesis